Small-angle neutron scattering studies of the effects of amphotericin B on phospholipid and phospholipid–sterol membrane structure

ARTICLE *in* BIOCHIMICA ET BIOPHYSICA ACTA · FEBRUARY 2011

Impact Factor: 4.66 · DOI: 10.1016/j.bbamem.2011.02.012 · Source: PubMed

6 AUTHORS, INCLUDING:

Fabrizia Foglia
Imperial College London
13 PUBLICATIONS **100** CITATIONS
SEE PROFILE

Alex F Drake
King's College London
72 PUBLICATIONS **1,173** CITATIONS
SEE PROFILE

Jayne Lawrence
King's College London
159 PUBLICATIONS **3,193** CITATIONS
SEE PROFILE

David Barlow
King's College London
131 PUBLICATIONS **3,957** CITATIONS
SEE PROFILE

Biochimica et Biophysica Acta 1808 (2011) 1574–1580

Contents lists available at ScienceDirect

Biochimica et Biophysica Acta

journal homepage: www.elsevier.com/locate/bbamem

Small-angle neutron scattering studies of the effects of amphotericin B on phospholipid and phospholipid–sterol membrane structure

F. Foglia [a], A.F. Drake [a], A.E. Terry [b], S.E. Rogers [b], M.J. Lawrence [a], D.J. Barlow [a,*]

[a] Pharmaceutical Science Division, Franklin Wilkins Building, King's College London, 150 Stamford Street, London SE1 9NH, UK
[b] ISIS Facility, STFC Rutherford Appleton Laboratory, Harwell Science & Innovation Campus, Didcot, OX11 0QX, UK

ARTICLE INFO

Article history:
Received 25 August 2010
Received in revised form 18 January 2011
Accepted 9 February 2011
Available online 18 February 2011

Keywords:
Phospholipid
POPC
Cholesterol
Ergosterol
Amphotericin
Lipid vesicles
Small-angle neutron scattering
Anti-fungal drugs
Circular dichroism

ABSTRACT

Small-angle neutron scattering (SANS) studies have been performed to study the structural changes induced in the membranes of vesicles prepared (by thin film evaporation) from phospholipid and mixed phospholipid–sterol mixtures, in the presence of different concentrations and different aggregation states of the anti-fungal drug, amphotericin B (AmB). In the majority of the experiments reported, the lipid vesicles were prepared with the drug added directly to the lipid dispersions dissolved in solvents favouring either AmB monomers or aggregates, and the vesicles then sonicated to a mean size of ~100 nm. Experiments were also performed, however, in which micellar dispersions of the drug were added to pre-formed lipid and lipid–sterol vesicles. The vesicles were prepared using the phospholipid palmitoyloleoylphosphatidylcholine (POPC), or mixtures of this lipid with either 30 mol% cholesterol or 30 mol% ergosterol. Analyses of the SANS data show that irrespective of the AmB concentration or aggregation state, there is an increase in the membrane thickness of both the pure POPC and the mixed POPC-sterol vesicles—in all cases amounting to ~4 Å. The structural changes induced by the drug's insertion into the model fungal cell membranes (as mimicked by POPC-ergosterol vesicles) are thus the same as those resulting from its insertion into the model mammalian cell membranes (as mimicked by POPC-cholesterol vesicles). It is concluded that the specificity of AmB for fungal *versus* human cells does not arise because of (static) structural differences between lipid–cholesterol-AmB and lipid–ergosterol-AmB membranes, but more likely results from differences in the kinetics of their transmembrane pore formation and/or because of enthalpic differences between the two types of sterol-AmB complexes.

1. Introduction

Over the past decade there has been a dramatic rise in the frequency of diagnosed fungal infections [1,2]—encompassing both systemic infections (ascribed to increased numbers of patients immuno-compromised through chemotherapy or HIV infection [2,3]) and also transplant- and implant-related infections (attributable to mycotic biofilm development [4]). This sharp increase in fungal infections has been accompanied by an increased frequency with which these infections prove recalcitrant to standard anti-fungal therapy [5–8]. There is an emerging demand, therefore, for novel anti-fungal agents that can circumvent the pathogens' resistance. The successful development of such novel anti-mycotics will clearly require an appreciation of both the mechanism(s) of action of the failed compounds and the molecular mechanism(s) underlying the reduced susceptibility of the resistant pathogens.

Since its discovery in the mid-1950s, one of the mainstays of the anti-fungal armamentarium has been the polyene macrolide antibiotic, amphotericin B (AmB) (Fig. 1) [3]. Several recent reports, however, have attested to the emergence of AmB-resistant strains of a number of clinically problematic pathogenic yeasts including *Candida* spp [1–8]. Now, although it has long been held that AmB exerts its anti-fungal action through the generation of self-assembled ion channels within the fungal cell membranes, there is no *direct structural* evidence to support this hypothesis. It has been shown that the selectivity of AmB for fungal vs. human cell membranes is linked to the organisms' differing steroid content—with fungal cell membranes having ergosterol and their mammalian counterparts, cholesterol. It has been proposed (on the basis of ion and non-electrolyte permeability studies) that AmB - and related polyene macrolides such as nystatin - forms ion channels within bio-membranes [9]. Models of these ion channels have been derived based upon a consideration of the amphipathic structures of the drugs, together with an experimental demonstration of their cooperativity in development of the toxigenic membrane conductance (which leads to cell death through indiscriminate transfer of ions across the cell membranes) [10]. The selective toxicity of AmB

* Corresponding author. Tel.: + 44 207 848 4827; fax: +44 207 848 4800.
E-mail addresses: fabrizia.foglia@kcl.ac.uk (F. Foglia), a.drake@kcl.ac.uk (A.F. Drake), ann.terry@stfc.ac.uk (A.E. Terry), sarah.rogers@stfc.ac.uk (S.E. Rogers), jayne.lawrence@kcl.ac.uk (M.J. Lawrence), dave.barlow@kcl.ac.uk (D.J. Barlow).

0005-2736/$ – see front matter © 2011 Elsevier B.V. All rights reserved.
doi:10.1016/j.bbamem.2011.02.012

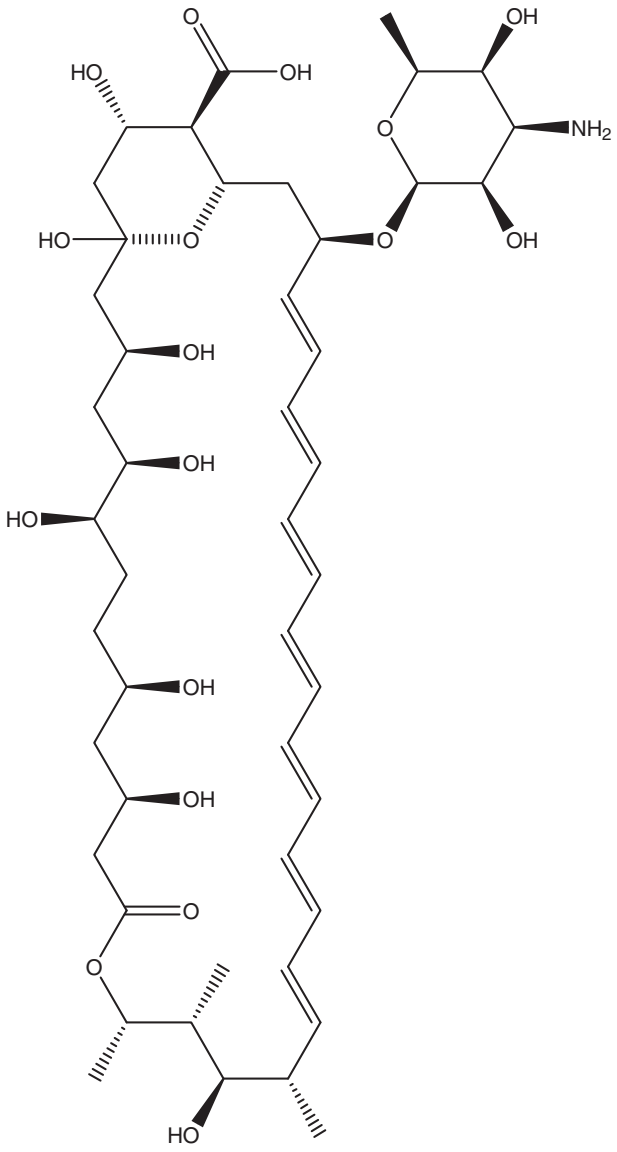

Fig. 1. Chemical structure of amphotericin B.

(and related polyene macrolide antibiotics) towards ergosterol-containing fungal cell membranes compared to cholesterol-containing human cell membranes is believed to be a crucial factor in the specificity for fungi, with the commonly held view that the ion channels formed involve drug-sterol complexation, with complexes involving ergosterol being strongly preferred over those involving cholesterol [11]. Recent research, however, suggests that this "textbook" explanation of how AmB works is only partially correct and very oversimplified [12–16]. It has been shown, for example, that the nature of the interaction between AmB and cell membranes is influenced very significantly by the concentration of drug [15,17,21–23], the concentration of sterol [17–19,23], and the lipid composition [20] and physical state/properties of the membrane [15,17,18]. Moreover, there is now controversy regarding the role of sterols in the membrane—and some experiments in fact indicate that AmB may form pores in sterol-free membranes [20–22]. Suffice to say, therefore, that there is considerable research effort still required to determine the molecular basis for the anti-mycotic activity of AmB and its related polyene antibiotics such as nystatin. Without a detailed understanding of the drugs' mechanism(s) of action, through which the chemistry of the drugs can be quantitatively related to their biological efficacy, it will prove difficult to develop novel variants of the drug which exhibit the necessary specificity, whilst also being effective against AmB-resistant fungi.

The information required to furnish such understanding can only be secured by using biophysical analytical techniques to probe, in a systematic way, the interactions between the drug, sterols and lipids at the molecular level. The first such studies – employing a combination of small-angle neutron scattering (SANS), X-ray diffraction and Fourier transform infrared spectroscopy – were reported by Hereć et al. [17]. In these studies, however, the membrane interactions of AmB were investigated using vesicles prepared from egg lecithin alone—*without* incorporated cholesterol or ergosterol [17].

Here, we report SANS studies performed on both phospholipid and phospholipid–sterol vesicles, as a means to securing an understanding of how differences in a sterol's structure influence its effects on biomembranes, and as a means also then to explore how these differences influence the membrane interactions of the polyene macrolide antibiotic AmB.

2. Materials and methods

2.1. Sample preparation

All chemicals – other than those indicated below – were purchased from Sigma-Aldrich Ltd. (Gillingham, UK) and were used as received. Hydrogenated and deuterated phospholipids were purchased from Avanti Polar Lipids (Alabaster, AL, USA). The dispersions of the vesicles were prepared by means of thin film evaporation [24]. For the majority of the experiments detailed below, phospholipid and 2:1 phospholipid–sterol solutions were prepared in chloroform (5 mL, Fluka, UK, Ltd., Dorset; spectroscopic grade) at a concentration of 1.25 mg/mL (or the equivalent in the case of *d*-lipid samples), and were evaporated to dryness using a BUCHI 461 rotary evaporator. The resulting *h*-lipid films were then dispersed in 5 mL D_2O (Aldrich, UK, Ltd., Dorset; 99.7% D), and the corresponding *d*-lipid films were dispersed either in H_2O or D_2O. These aqueous lipid dispersions were vortexed for 5 min, placed in a water bath at ambient temperature for 10 min, and finally ultrasonicated for 5 min using a probe sonicator (Lucas Dawes Ultrasonicator Soniprobe). (The concentration of the lipid dispersions was ~1.25 mg/mL – with the precise concentration dependent on the particular lipid/lipid:sterol mixture used – and so the molar ratio of water:lipid was always in excess of 30:1.) Equivalent sets of samples were also prepared incorporating a final concentration of AmB in the lipid film of 0.1 μM, 1 μM, 10 μM or 100 μM. For these latter samples, the AmB was initially prepared as a 25 mg/mL stock solution in dimethyl sulfoxide (DMSO, Fluka, UK, Ltd., Dorset; spectroscopic grade), and the required volume of this stock then taken and added to the lipid or lipid:sterol solution dissolved in chloroform or chloroform:methanol 2:1 v/v. (The latter was employed in the case of the systems involving 10 μM and 100 μM AmB as a precaution against aggregation of the drug.) [25]. The level of DMSO in the final aqueous dispersions of these AmB-containing vesicles was always ≤0.04 vol%. Other samples were also prepared with an aqueous dispersion of AmB (containing ≤0.04 vol% DMSO) added to pre-formed lipid or lipid–sterol vesicles; for these experiments the AmB and lipid (or lipid–sterol) solutions (in either D_2O or H_2O) were prepared at twice the required final concentration (*viz.*, ~2.5 mg/mL for the lipid, and 200 μM for the AmB), and the samples then prepared by mixing the drug and vesicle stocks in the ratio 1:1. For each vesicle suspension (diluted from the corresponding solution used for SANS studies by 1 in 16) photon correlation spectroscopic (PCS) measurements were recorded as a function of time (using a Brookhaven Zetaplus instrument), and indicated that the dispersions were stable (at ambient temperature) for up to 3 days (the time required to perform the SANS experiments), showing no significant change in particle size or polydispersity over this period (typically

~100 nm and ~0.15 for the POPC samples, and ~100 nm and ~0.18 for the mixed POPC-sterol samples). For all samples, the resulting preparations gave vesicle volume fractions ≤ 0.005, (assuming only ULVs of uniform diameter 100 nm) and the solvent used in preparation caused no discernable changes in the vesicle size distribution or stability. Note, too, that the vesicle samples were *not* centrifuged following ultrasonication, because any particles shed by the titanium probe would be far too large to interfere with the subsequent SANS measurements.

2.2. SANS measurements and data analysis

SANS measurements were performed on the LOQ beam line at the ISIS pulsed neutron source (STFC Rutherford Appleton Laboratory, Didcot, UK). LOQ uses pulses of neutrons with wavelengths 2.2 to 10 Å which are separated by time-of-flight and recorded at a 64 cm^2, two-dimensional ^{3}H-CF_4 detector (ORDELA Inc., Oak Ridge, USA) at 4.1 m from the sample. Wavelength-dependent corrections are made to allow for the incident spectrum, detector efficiencies, and measured sample transmissions to create a composite SANS pattern (as described in detail in Heenan et al. [26]). This setup gives a scattering vector $Q = (4\pi/\lambda)\sin(\theta)$ range of 0.008 $Å^{-1}$ to 0.22 $Å^{-1}$. Comparisons with scattering from a partially deuterated polystyrene standard allow absolute scattering cross sections to be determined, with an error of around 2%. Samples were placed in disk-shaped fused silica cells of 1.0 mm (for H_2O) or 2.0 mm (for D_2O) path length (Hellma UK, Ltd., Essex). All SANS measurements were recorded with samples maintained at 298 K, using a 12-mm-diameter neutron beam. Backgrounds from pure H_2O or D_2O were subtracted. All fitting procedures included flat background corrections to allow for any mismatch in the incoherent and inelastic scattering between sample and solvent. Fitted background levels were always checked to determine whether they were of a physically reasonable magnitude. Given that PCS measurements indicated that the vesicles in all samples were ~100 nm diameter, and in each case, therefore, could safely be assumed to involve a mixture of predominantly multilamellar with some unilamellar vesicles, the SANS data were modelled as previously [27,28], assuming mixtures of (isolated) infinite planar sheets and 1-dimensional paracrystalline stacks of these [29–31], with the various model parameters optimised using Heenan's FISH software [32].

3. Results and discussion

For each of the pure lipid and mixed lipid–sterol systems investigated, the SANS data were recorded (at 298 K) in the absence of amphotericin (AmB) and in the presence of different final concentrations of AmB in the range 0.1–100 μM (the cmc of the drug being 1 μM [33]). For each system (with the exception of the system involving 0.1 μM AmB, where only the *h*-lipid system was studied), the SANS data were obtained under three different H/D contrasts provided by *h*-lipid vesicles dispersed in D_2O, and *d*-lipid vesicles dispersed in D_2O or H_2O. Simultaneous model fits to these data were obtained as described previously [30,31] using the FISH program [32]. The parameters refined in the model fitting included the sample background scattering, the proportions of unilamellar vesicles (ULVs) and multilamellar vesicles (MLVs), the thickness of the vesicle lamellae (L, Å; taken to be the same for the ULVs and MLVs), the *d*-spacing of the MLVs (D, Å) and the polydispersity on the *d*-spacing ($\sigma(D)/D$). Three other parameters involved in the SANS models were initially treated as adjustable - and were thus fitted along with the six parameters listed above - but preliminary analyses revealed that their fitted values showed insignificant variation from dataset to dataset; in the final analyses, therefore, these parameters were constrained as fixed. These fixed parameters (and their constrained values) included the polydispersity on the thickness of the vesicle lamellae ($\sigma(L)/L$; taken as zero – but of practical necessity input as 10^{-6}), the mean lamellarity of the MLVs in the sample (M; 3), and the Lorentz correction factor ($R\sigma$; 236 Å) [28]. The fitted parameter values for all systems studied are summarised in Table 1, and illustrative SANS data together with the corresponding model fits are shown in Figs. 2–4.

For the pure POPC vesicle preparations, the model fits to the SANS data (Fig. 2) indicate a mixture of ULVs and MLVs, with a lamellar thickness, $L = 36.5 \pm 0.2$ Å (Table 1). For comparison, we note that Kučerka et al. [34] give the Luzatti thickness for oriented (hydrated) POPC bilayer stacks as 36.8 Å. For the MLVs in these pure POPC samples, the *d*-spacing has a fitted value of 56.1 Å, with a statistical uncertainty of ±0.3 Å. Here, however, as with all of the systems described below, the uncertainty in the estimated *d*-spacing is not given just by the statistical uncertainty in the position of the Gaussian peak (D), but by the convolution of this with the width of the Gaussian distribution ($\sigma(D)$). The true uncertainty in the *d*-spacing for the POPC

Table 1
Structural parameters obtained through simultaneous fits to the three sets of SANS data obtained for vesicle dispersions prepared from the various phospholipid and phospholipid–sterol mixtures in the absence and presence of amphotericin (AmB). Symbols used are as described in the text.

Lipid(s)	Solvent[a]	[AmB]/μM	L[b]/Å	D[b]/Å	Ratio of ULV:MLV surface areas[c]		
					h− in D_2O	*d*− in D_2O	*d*− in H_2O
POPC	$CHCl_3$	0	36.5 (0.3)	56.1 ± 8	2.1	1.7	3.1
		0.1	39.7 (0.2)	59.8 ± 3	1.9	–	–
		1	40.1 (0.3)	61.9 ± 3	2.1	1.6	2.8
	$CHCl_3$:MeOH	10	39.5 (0.3)	59.4 ± 3	1.8	1.5	0.9
		100	39.5 (0.3)	60.0 ± 3	1.6	1.6	1.9
POPC-Chol	$CHCl_3$	0	41.4 (0.3)	56.1 ± 3	2.1	1.9	1.6
		0.1	43.7 (0.6)	62.4 ± 4	1.5	–	–
		1	43.7 (0.3)	62.0 ± 4	1.6	1.3	3.4
	$CHCl_3$:MeOH	10	43.7 (0.3)	62.4 ± 4	1.6	1.8	2.2
		100	43.7 (0.2)	62.4 ± 4	1.7	1.6	1.7
POPC-Erg	$CHCl_3$	0	40.7 (0.3)	56.5 ± 4	2.1	2.2	1.4
		0.1	43.7 (0.4)	62.4 ± 4	2.6	–	–
		1	43.7 (0.3)	62.4 ± 4	1.8	1.5	2.0
	$CHCl_3$:MeOH	10	43.7 (0.2)	62.4 ± 4	2.2	1.8	3.9
		100	43.7 (0.6)	62.4 ± 4	1.7	1.5	0.4

[a] For L, the figures in parentheses show standard errors; for D, the uncertainties reported represent the convolution of the statistical error on D and the value of the fitted polydispersity.
[b] Samples prepared using only lipid or lipid–sterol mixtures with AmB at a concentration of 0–1 μM were prepared in $CHCl_3$, whilst those incorporating AmB at concentrations of 10 μM and 100 μM were prepared in $CHCl_3$:MeOH—as a means to ensure that the drug was not aggregated (see Supplementary information).
[c] Dashes in the final two columns indicate systems for which SANS measurements were not recorded.

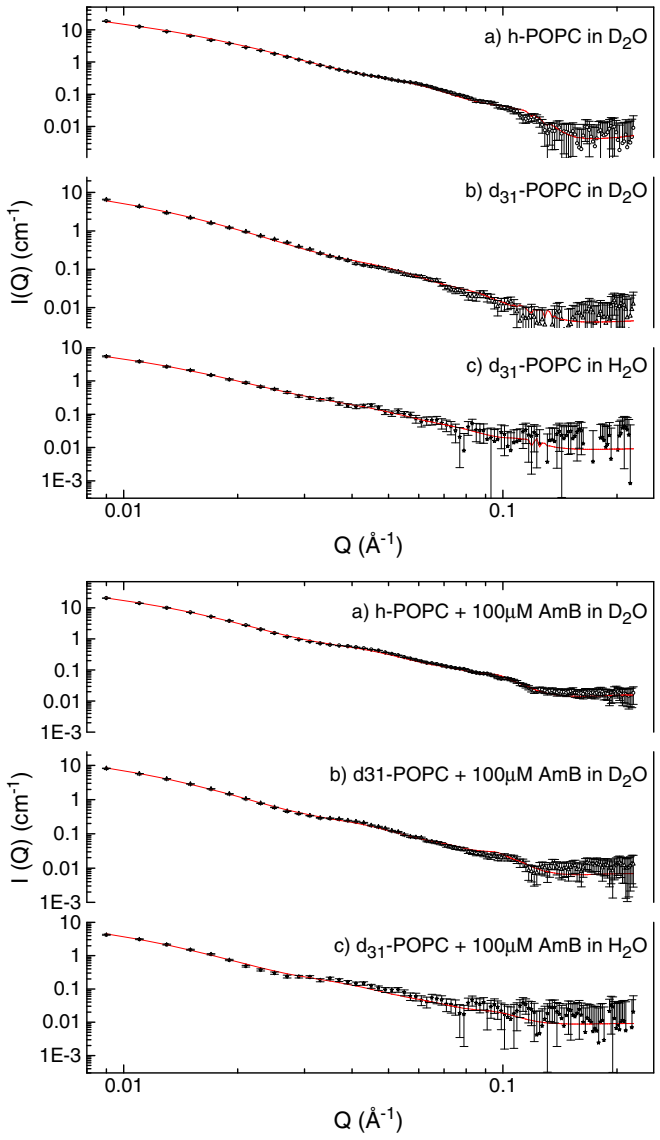

Fig. 2. SANS data and model fits for POPC vesicles in the absence of AmB (upper panel) and with the incorporation of 100 μM AmB in the lipid film used in preparation of the vesicle dispersion (lower panel). Q is the neutron momentum transfer, in $Å^{-1}$. The structural parameters for the model fits shown are presented in Table 1.

MLVs is thus obtained as ±8 Å. We note, therefore, that although the SANS data cannot be satisfactorily modelled assuming ULVs alone—the fitting for all systems warranting consideration of a mixed population of MLVs and ULVs, the precision on the MLV *d*-spacing is rather poor (for the pure POPC MLVs, 49–65 Å). Such imprecision is sadly inevitable given the absence of a clear Bragg peak in the SANS profile. It is encouraging nevertheless to note that this *d*-spacing range does span the values previously reported for POPC vesicles and multilayers (typically, 54–65 Å [34–37]).

Using the bilayer thickness data together with the lipid molecular volumes (v_L, taken from Greenwood et al. [38]; see Table 2) the mean lipid interfacial area can be calculated as $a_0 = 2v_L/L$ [39]. For the POPC vesicle bilayers, such calculations give $a_0 = 68.8 \pm 0.4$ $Å^2$, which is consistent with the value reported by Kučerka et al. [34] on the basis of X-ray diffraction measurements on oriented POPC bilayer stacks (*viz.*, $a_0 = 68.3$ $Å^2$).

When the POPC vesicles are prepared in the presence of 30 mol% sterol, the SANS data (*cf.* Figs. 3, 4) model fits (Table 1) show that the bilayer thickness increases by ~4 Å for added ergosterol, and ~5 Å for added cholesterol, although - given the experimental uncertainties of ±0.3 Å - the difference for the two sterols here is probably not significant. These results are consistent with the findings of other workers, with the ^{2}H-NMR studies of Nezil and Bloom [40] giving a 4 Å increase in thickness of the hydrophobe region of POPC bilayers in the presence of 30 mol% cholesterol.

Using the thickness estimates for the mixed lipid–sterol bilayers we can again calculate the effective lipid interfacial molecular areas, a_0. In this case, however, it is necessary to employ molecular volumes computed as the mean of the lipid and sterol (Table 2 [38,41]), weighted according to their mole fraction in the mixture. For the POPC-cholesterol and POPC-ergosterol bilayers, we have $v_L = (0.7 \times 1256) + (0.3 \times 623) = 1066$ $Å^3$, and $v_L = (0.7 \times 1256) + (0.3 \times 608) = 1062$ $Å^3$, respectively. The corresponding mean molecular areas are then obtained as $a_0 \approx (2 \times 1064)/41 = 52$ $Å^2$. Now, if the mean molecular areas are computed instead using the weighted mean of the bilayer interfacial areas for the pure lipid and that for (chole) sterol (27 $Å^2$; [42]) we get $a_0 = 59.6$ $Å^2$ for the POPC-sterol bilayers. Accordingly, the (known) condensing effect of the sterols on the

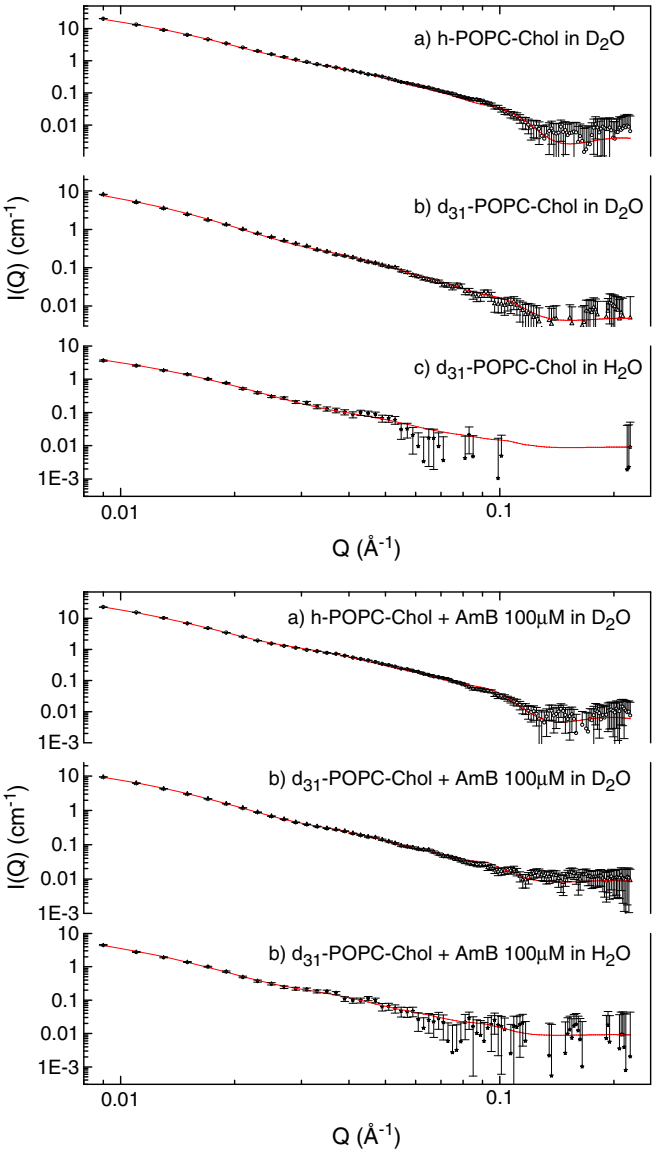

Fig. 3. SANS data and model fits for POPC-cholesterol vesicles in the absence of AmB (upper panel) and with incorporation of 100 μM AmB in the lipid film used in preparation of the vesicle dispersion (lower panel). Q is the neutron momentum transfer, in $Å^{-1}$. The structural parameters for the model fits shown are presented in Table 1.

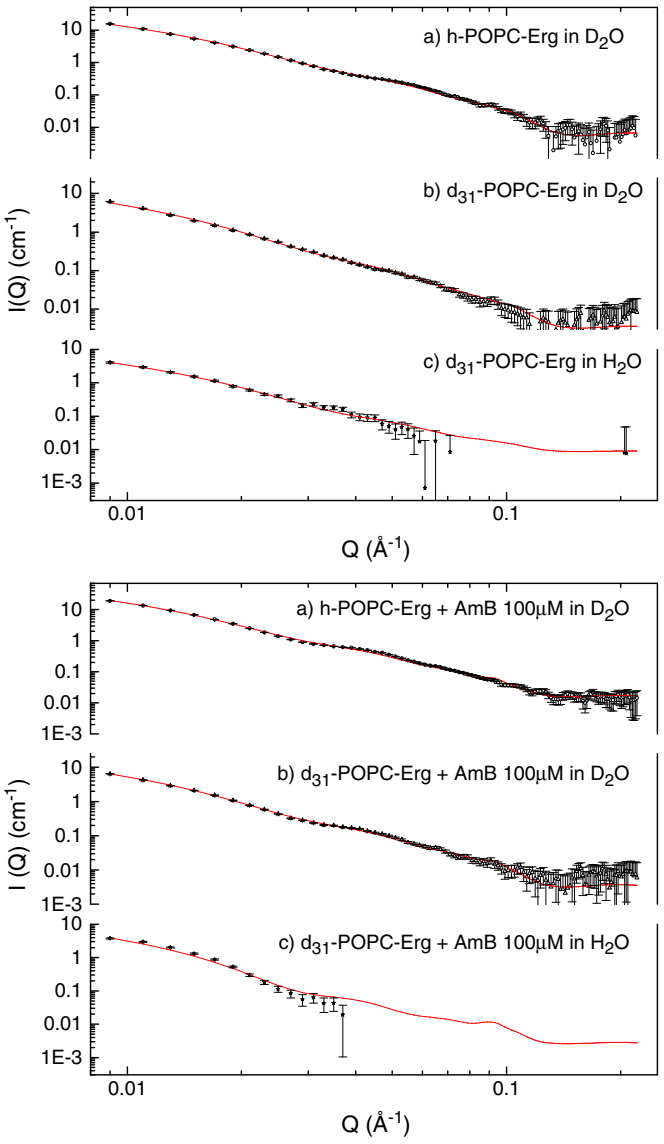

Fig. 4. SANS data and model fits for POPC-ergosterol vesicles in the absence of AmB (upper panel) and with incorporation of 100 μM AmB in the lipid film used in preparation of the vesicle dispersion (lower panel). Q is the neutron momentum transfer, in $Å^{-1}$. The structural parameters for the model fits shown are presented in Table 1.

phospholipid bilayers amounts to a 18% condensation, which is close to the figure of 12% reported for the cholesterol-induced condensation of POPC monolayers maintained at a surface pressure of 30 mN/m [43].

When amphotericin (AmB) is added to the lipid films in the course of preparing the vesicles, the effect on the vesicle bilayer structure seems independent of the vesicle composition. In the case of the SANS data for the vesicles prepared from POPC alone (Fig. 3), the model fits (Table 1) indicate that the presence of AmB seems to cause a small increase in the bilayer thickness, from ~37 Å to ~40 Å. This change is consistent with the structural/spectroscopic studies reported by Umegawa et al. [44] which indicated the formation of AmB aggregates in POPC membranes; they also accord with the earlier observations made in H^+ release experiments which show that phospholipid vesicles are sensitive to AmB even in the absence of sterols [45]. Although Hereć et al. [46] reported no change in bilayer thickness caused by the addition of AmB to egg yolk phosphatidylcholine vesicles, this was only for AmB concentrations at or below 1 mol%, and the authors do note that at an AmB concentration of 5 mol%, there is a significant change in the lipid acyl chain ordering which is consistent with an incorporation of the drug into the hydrophobe layer of the membrane. (In the samples studied here – assuming that all of the added drug remains in the vesicle membranes - the use of 100 μM AmB equates to an addition of the drug at 3 mol%.)

If either (30 mol%) cholesterol or ergosterol is included in the POPC bilayers, the SANS data (*cf.* Figs. 3 and 4) model fits (Table 1) indicate that the addition of AmB causes the same increase in thickness as seen with POPC vesicles - amounting to ~3 Å. This increase in thickness might arise because (1) AmB simply embeds itself within the lipid head groups and lies more or less flat on the membrane surface, or (2) AmB inserts itself vertically into the outer leaflet of the bilayer with its amino-sugar head group protruding slightly above the level of the phosphocholine head groups. On the basis of the SANS data modeling performed here, there is no direct way to distinguish these two situations. However, by analogy with the situation found to pertain for membrane active anti-microbial peptides (for example, protegrin [47]), it might be expected that the binding of the polyene macrolide AmB within the lipid head groups would actually lead to a disturbance of the lipid packing and thence to membrane *thinning* and not - as seen here – membrane *thickening*. Also, given that AmB induces the same changes in the vesicle membranes regardless of whether the drug is added at a concentration below or above its cmc (1 μM [33]), it seems most likely that the increase in vesicle membrane thickness arises due to a vertical insertion of the drug into the membrane. If this were not to be the case then the AmB micelles would first need to dissociate in order to liberate AmB monomers which could then migrate and spread across the membrane surface, and such a situation seems energetically very unlikely. Moreover, a vertical insertion of AmB into the membrane is clearly indicated by the fluorescence measurements presented by Silva et al. [48] which showed significant sterol structure-dependent differences in the transmembrane ion currents induced by the related polyene macrolide antibiotic, nystatin, and also by the DSC and FT-IR

Table 2
Volumes and densities of POPC, ergosterol, cholesterol, and amphotericin (quoted for the temperature indicated).

Compound	Temperature/K	Volume/$Å^3$	Density/g cm^{-3}
POPC [38]	303	1256	0.995
Cholesterol [38]	298	623	0.94
Ergosterol [41]	298	608	0.92
Amphotericin B [50]	298	983	1.56

Table 3
Structural parameters obtained through model fitting of SANS data recorded at various times after injection of amphotericin (to a final concentration of 100 μM) into pre-formed *h*-lipid vesicle dispersions prepared (in D_2O) from the various phospholipid and phospholipid–sterol mixtures. Symbols used are as described in the text, and the figures in parentheses show standard errors.

Lipid(s)	[AmB]/μM	Time from injection	L^a/Å	D^a/Å	Ratio of ULV:MLV surface areas
					h— in D_2O
POPC	0	0	37.6 (0.3)	51.4 ± 3	3.1
	10	39 min	39.5 (0.4)	60.0 ± 3	1.6
	100	25 h 15 min	39.5 (0.3)	60.0 ± 3	1.7
POPC-Chol	0	0	42.0 (0.3)	57.4 ± 3	1.6
	10	36 min	44.0 (0.3)	62.0 ± 4	1.6
	100	24 h 18 min	44.0 (0.4)	62. 0 ± 4	1.6
POPC-Erg	0	0	41.0 (0.4)	55.2 ± 4	2.2
	10	39 min	44.8 (0.3)	62.3 ± 4	2.0
	100	24 h	44.0 (0.6)	63. 0 ± 4	2.0

[a] For *L*, the figures in parentheses show standard errors; for *D*, the uncertainties reported represent the convolution of the statistical error on *D* and the value of the fitted polydispersity.

data presented by Fournier et al. [49] showing direct interaction between the hydrophobes of AmB and ergosterol.

It is important to note, however, that in the SANS experiments described above, the AmB (for reasons of simplicity) was incorporated directly into the vesicle bilayers through its inclusion in the lipid films used in preparation of the vesicles. It is perfectly possible, therefore, that the structural information derived in these experiments could be entirely irrelevant to the *in vivo* situation—where the drug partitions into the cell membranes from its dispersion (as monomers and/or aggregates) in the bulk. In order to determine whether such membrane-bulk AmB interactions would lead to the formation of the same membrane structures as reported above, we thus performed a more limited set of experiments in which the drug was mixed with pre-formed lipid and lipid–sterol vesicles, and the SANS profiles of these systems were monitored and modelled as a function of time after mixing. The model fits to these SANS curves (with the values of the fitted parameters summarised in Table 3) clearly show that the structures of the membranes resulting from the interaction of AmB with pre-formed vesicles seem to be exactly the same as found for those where the drug was embedded in the membranes at the time of vesicle formation. Indeed, the changes in bilayer thickness and multilayer *d*-spacings seem to be complete within one hour of mixing of the drug and vesicles (the shortest measurement interval that was possible given the experimental conditions; Table 3)—and again the resulting membrane structures are no different for the POPC-cholesterol and the POPC-ergosterol membranes.

4. Conclusions

The specificity of AmB for fungal *versus* human cells would thus seem to arise not because of any static structural differences between lipid–cholesterol-AmB and lipid–ergosterol-AmB membranes, but more likely because of differences in the kinetics of their transmembrane pore formation and/or because of enthalpic differences between the two types of sterol-AmB complexes, which then manifest as differences in the life-times and/or distributions of the two types of complex within the plane of the membrane.

Appendix A. Supplementary data

Supplementary data to this article can be found online at doi:10.1016/j.bbamem.2011.02.012.

References

[1] M.A. Pfaller, D.J. Diekema, Epidemiology of invasive candidiasis: a persistent public health problem, Clin. Microbiol. Rev. 20 (2007) 133–163.
[2] T.C. White, K.A. Marr, R.A. Bowden, Clinical, cellular, and molecular factors that contribute to antifungal drug resistance, Clin. Microbiol. Rev. 11 (1998) 382–402.
[3] S. Sundriyal, R.K. Sharma, R. Jain, Current advances in antifungal targets and drug development, Curr. Med. Chem. 13 (2006) 1321–1335.
[4] G. Ramage, J.P. Martinez, J.L. Lopez-Ripot, Candida biofilms on implanted biomaterials: a clinically significant problem, FEMS Yeast Res. 6 (2006) 979–986.
[5] M.D. LaFleur, C.A. Kumamoto, K. Lewis, Candida albicans biofilms produce antifungal-tolerant persister cells, Antimicrob. Agents Chemother. 50 (2006) 3839–3846.
[6] H. Vanden Bossche, F. Dromer, I. Improvisi, M. Lozano-Chiu, J.H. Rex, D. Sanglard, Antifungal drug resistance in pathogenic fungi, Med. Mycol. 36 (1998) 119–128.
[7] P. Vandeputte, G. Tronchin, T. Berges, C. Hennequin, D. Chabasse, J.P. Bouchara, Reduced susceptibility to polyenes associated with a missense mutation in the ERG6 gene in a clinical isolate of *Candida glabrata* with pseudohyphal growth, Antimicrob Agents Chemother. 51 (2007) 982–990.
[8] J. Nett, L. Lincoln, K. Marchillo, R. Massey, K. Holoyda, B. Hoff, M. VanHandel, D. Andes, Putative role of beta-1, 3 glucans in *Candida albicans* biofilm resistance, Antimicrob. Agents Chemother. 51 (2007) 510–520.
[9] A. Finkelstein, R. Holz, Aqueous pores created in thin lipid membranes by the polyene antibiotics nystatin and amphotericin B, Membranes 2 (1973) 377–378.
[10] A.W. Norman, R.A. Demel, B. De Kruyff, W.S.M.G. Van Kessel, L.L.M. Van Deenen, Studies on the biological properties of polyene antibiotics: comparison of other polyenes with filipin in their ability to interact specifically with sterol, Biochim. Biophys. Acta 290 (1972) 1–14.
[11] T.E. Andreoli, Structure and function of Amphotericin B-Cholestrol pores in lipid bilayer membranes, Ann. NY Acad. Sci. 235 (1974) 448–468.
[12] H.W. Katarzyna, D.L. Patrycja, Interaction between nystatin and natural membrane lipids in Langmuir monolayers—the role of a phospholipid in the mechanism of polyenes mode of action, Biophys. Chem. 123 (2006) 154–161.
[13] J. Minones, O. Conde, P. Dynarowicz-Latka, M. Casas, Penetration of amphotericin B into DOPC monolayers containing sterols of cellular membranes, Colloids Surf. A 270 (2005) 129–137.
[14] M. Gagos, J. Gabrielska, M. Dalla Serra, W.I. Gruszecki, Binding of antibiotic amphotericin B to lipid membranes: monomolecular layer technique and linear dichroism-FTIR studies, Mol. Membr. Biol. 22 (2005) 433–442.
[15] B.V. Cotero, S. Rebolledo-Antunez, I. Ortega-Blake, On the role of sterol in the formation of the amphotericin B channel, Biochim. Biophys. Acta 1375 (1998) 43–51.
[16] M.M. Wang, I.P. Sugar, P.L.G. Chong, Role of the sterol superlattice in the partitioning of the antifungal drug nystatin into lipid membranes, Biochem. 37 (1998) 11797–11805.
[17] M. Herec, A. Islamov, A. Kuklin, M. Gagoś, W.I. Gruszecki, Effect of antibiotic amphotericin B on structural and dynamic properties of lipid membranes formed with egg yolk phosphatidylcholine, Chem. Phys. Lipids 147 (2007) 78–86.
[18] B. Venegas, J. González-Damián, H. Celis, I. Ortega-Blake, Amphotericin B channels in the bacterial membrane: role of sterol and temperature, Biophys. J. 85 (2003) 2323–2332.
[19] B.E. Cohen, A sequential mechanism for the formation of aqueous channels by amphotericin-B in liposomes—the effect of sterols and phospholipid-composition, Biochim. Biophys. Acta 1108 (1992) 49–58.
[20] T. Ruckwardt, A. Scott, J. Scott, P. Mikulecky, S.C. Hartsel, Lipid and stress dependence of amphotericin B ion selective channels in sterol-free membranes, Biochim. Biophys. Acta 1372 (1998) 283–288.
[21] I. Fournier, J. Barwicz, P. Tancrede, The structuring effects of amphotericin B on pure and ergosterol- or cholesterol-containing dipalmitoylphosphatidylcholine bilayers: a differential scanning calorimetry study, Biochim. Biophys. Acta 1373 (1998) 76–86.
[22] B.D. Wolf, S.C. Hartsel, Osmotic-stress sensitises sterol-free phospholipid-bilayers to the action of amphotericin-B, Biochim. Biophys. Acta 1238 (1995) 156–162.
[23] M.J. Paquet, I. Fournier, J. Barwicz, P. Tancrède, M. Auger, The effect of amphotericin B on pure ergosterol- or cholesterol-containing dipalmitoylphosphatidylcholine bilayers as viewed by ^{2}H NMR, Chem. Phys. Lipid 119 (2002) 1–11.
[24] C.J. Kirby, G. Gregoriadis, Liposome Technology, in: G. Gregoriadis (Ed.), CRC Press, Boca Raton, FL, 1984, pp. 19–22.
[25] J. Bolard, M. Seigneuret, G. Boudet, Interaction between phospholipid-bilayer membranes and the polyene antibiotic amphotericin-B – lipid state and cholesterol content dependence, Biochim. Biophys. Acta 599 (1980) 280–293.
[26] R.K. Heenan, J. Penfold, S.M. King, SANS at pulsed neutron sources: present and future prospects, J. Appl. Cryst. 30 (1997) 1140–1147.
[27] G. Ma, D.J. Barlow, M.J. Lawrence, R.K. Heenan, P. Timmins, -angle neutron-scattering studies of nonionic surfactant vesicles, J. Phys. Chem. B 104 (2000) 9081–9085.
[28] R.D. Harvey, R.K. Heenan, D.J. Barlow, M.J. Lawrence, The effect of electrolyte on the morphology of vesicles composed of the dialkyl polyoxyethylene ether surfactant 2C(18)E(12), Chem. Phys. Lipids 13 (2005) 27–36.
[29] M. Kotlarchyk, S.M. Ritzau, Paracrystal model of the high-temperature lamellar phase of a ternary microemulsion system, J. Appl. Cryst. 24 (1991) 753–758.
[30] M. Shibayama, T. Hashimoto, Small-angle X-ray-scattering analyses of lamellar microdomains based on a model of one-dimensional paracrystal with uniaxial orientation, Macromolecules 19 (1986) 740–749.
[31] N.T. Skipper, A.K. Soper, J.D.C. McConnell, The structure of interlayer water in vermiculite, J. Chem. Phys. 94 (1991) 5751–5760.
[32] R.K. Heenan, RAL Report 89–129, as subsequently revised; Rutherford Appleton Laboratory: Didcot, U.K., 1989.
[33] P. Tancrede, J. Barwicz, S. Jutras, I. Gruda, The effect of surfactants on the aggregation state of amphotericin B, Biochim. Biophys. Acta 1030 (1990) 289–295.
[34] N. Kučerka, S. Tristram-Nagle, J.F. Nagle, Structure of fully hydrated fluid phase lipid bilayers with monounsaturated chains, J. Membr. Biol. 208 (2005) 193–202.
[35] K. Gawrisch, H.C. Gaede, M. Mihailescu, S.H. White, Hydration of POPC bilayers studied by H-1-PFG-MAS-NOESY and neutron diffraction, Eur. Biophys. J. 36 (2007) 281–291.
[36] H. Schmiedel, L. Almasy, G. Klose, Multilamellarity, structure and hydration of extruded POPC vesicles by SANS, Eur. Biophys. J. 35 (2006) 181–189.
[37] G. Pabst, M. Rappolt, H. Amenitsch, P. Laggner, Structural information from multilamellar liposomes at full hydration: full Q-range fitting with high quality X-ray data, Phys. Rev. E 62 (2000) 4000–4009.
[38] A.I. Greenwood, S. Tristram-Nagle, J.F. Nagle, Partial molecular volumes of lipids and cholesterol, Chem. Phys. Lipids 143 (2006) 1–10.
[39] B.A. Lewis, D.M. Engelman, Lipid bilayer thickness varies linearly with acyl chain-length in fluid phosphatidylcholine vesicles, J. Mol. Biol. 166 (1983) 211–217.
[40] F.A. Nezil, M. Bloom, Combined influence of cholesterol and syntetic amphiphillic peptides upon bilayer thickness in model membranes, Biophys. J. 61 (1992) 1176–1183.
[41] D.R. Lide, CRC Handbook of Chemistry & Physics, CRC Press Inc, Boca Raton, Florida, USA, 2009.
[42] J. Pan, S. Tristram-Nagle, J.F. Nagle, Effect of cholesterol on structural and mechanical properties of membranes depends on lipid chain saturation, Phys. Rev. E 80 (2009) 021931.
[43] J.M. Smaby, M.M. Momsen, H.L. Brockman, R.E. Brown, Phosphatidylcholine acyl unsaturation modulates the decrease in interfacial elasticity induced by cholesterol, Biophys. J. 73 (1997) 1492–1505.

[44] Y. Umegawa, N. Matsumori, T. Oishi, T. Murata, Ergosterol increases the intermolecular distance of Amphotericin B in the membrane-bound assembly as evidenced by solid-state NMR, Biochem. 47 (2008) 13463–13469.
[45] A. Vertut-Croquin, J. Bolard, M. Chabbert, C. Gary-Bobo, Differences in the interaction of the polyene antibiotic amphotericin-B with cholesterol-containing or ergosterol-containing phospholipid-vesicles—a circular-dichroism and permeability study, Biochem. 22 (1983) 2739–2744.
[46] M. Hereć, A. Islamov, A. Kuklin, M. Gagoś, W.I. Gruszecki, Effect of antibiotic amphotericin B on structural and dynamic properties of lipid membranes formed with egg yolk phosphatidylcholine, Chem. Phys. Lipids 147 (2007) 78–86.
[47] W.T. Heller, A.J. Waring, R.I. Lehrer, T.A. Harroun, T.M. Weiss, L. Yang, H.W. Huang, Membrane thinning effect of the b-sheet antimicrobial protegrin, Biochemistry 39 (2000) 139–145.
[48] L. Silva, A. Coutinho, A. Fedorov, M. Priteo, Competitive binding of cholesterol and ergosterol to the polyene antibiotic Nystatin. A fluorescence study, Biophys. J. 90 (2006) 3625–3631.
[49] I. Fournier, J. Barwicz, M. Auger, P. Tancrède, The chain conformational order of ergosterol- or cholesterol-containing DPPC bilayers as modulated by Amphotericin B: a FTIR study, Chem. Phys. Lipids 151 (2008) 41–50.
[50] J. Kirschbaum, S.G. Kahn, Micelle size and stability of aqueous amphotericin B (polyene) systems, J. Pharm. Sci. 56 (1967) 278–279.